RSC Advances

PAPER

View Article Online
View Journal | View Issue

Cite this: *RSC Adv.*, 2021, **11**, 9403

Ligand-based pharmacophore modeling, virtual screening and biological evaluation to identify novel TGR5 agonists†

Shizhen Zhao,[a] Xinping Li,[a] Wenjing Peng,[a] Le Wang,[a] Wenling Ye,[a] Yang Zhao,[a] Wenbo Yin,[c] Wei-Dong Chen,[ab] Weiguo Li*[a] and Yan-Dong Wang*[d]

Received 2nd December 2020
Accepted 19th February 2021

DOI: 10.1039/d0ra10168k

rsc.li/rsc-advances

Takeda G-protein-coupled receptor 5 (TGR5) is emerging as an important and promising target for the development of anti-diabetic drugs. To understand the structural characteristics of TGR5 agonists, the common feature pharmacophore models were generated and molecular docking was performed. The ligand-based virtual screening combined with pharmacophore mapping and molecular docking was performed to identify novel nonsteroidal TGR5 agonists. Finally, 20 compounds were screened for *in vitro* TGR5 agonistic activity assay, and results showed most compounds exhibiting TGR5 agonistic activity at 40 μM. Among these compounds, **V12** and **V14** displayed obvious TGR5 agonist activity, with the EC_{50} values of 19.5 μM and 7.7 μM, respectively. Compounds **V12** and **V14** could be considered potential TGR5 agonist candidates and also may be used as initial hits for developing novel TGR5 agonists.

1. Introduction

Takeda G-protein-coupled receptor 5 (TGR5) belongs to the G-protein coupled receptor family and was first identified as a bile acid receptor in 2002.[1,2] TGR5 is widely expressed in the gallbladder, placenta, spleen, and intestine.[3] The activation of TGR5 can cause an increase of glucagon-like peptide-1 (GLP-1), which activates intestinal cell secretion and plays a key role in glucose metabolism and energy homeostasis.[4–6] In addition, TGR5 activation promotes energy expenditure in brown adipose tissue and muscle by increasing the basal metabolic rate.[4,7] Therefore, TGR5 has emerged as an attractive therapeutic target for the treatment of metabolic disorders, such as non-alcoholic steatohepatitis, type 2 diabetes mellitus (T2DM), and obesity.[8,9]

Medicinal chemistry approaches have discovered a variety of TGR5 agonists (Fig. 1). These agonists can be divided into two categories: steroidal and nonsteroidal agonists. The first series is structurally based on bile acids (BAs), including cholic acid (CA),[10] lithocholic acid (LCA),[11] and their semisynthetic derivatives such as 6α-ethyl-23(*S*)-methylcholic acid (INT-777, **a**).[12] The second series of TGR5 agonists includes some small synthetic molecules, such as [2-(2,5-dichlorophenoxy)pyridin-3-yl]-(3,4-dihydro-2*H*-quinolin-1-yl)methanone (**b**) and 4-(3,5-bis(trifluoromethyl)benzyl)-6-(2-fluorophen-yl)-4,5-dihydropyrido[3,2-*f*][1,4] oxazepin-3(2*H*)-one (**c**).[13,14] These compounds possess excellent agonistic properties and are effective in the treatment of nonalcoholic steatohepatitis, hypercholesterolemia, hypertriglyceridemia, and T2DM.[15]

The aim of this study is to identify novel nonsteroidal TGR5 agonists through a computer-aided drug discovery approach. The ligand-based pharmacophore modeling and molecular docking were performed to determine the structural characteristics and binding modalities of the TGR5 agonists. Then the selected pharmacophore hypotheses were used to screen the FDA approved database, Specs, TargetMol and in our library databases. Further screening of the retrieved compounds was performed using molecular docking. Finally, 20 commercially available hit compounds were selected by our virtual screening approach, and evaluated for their *in vitro* TGR5 agonistic activity assay. Overall, the results of our study are expected to be useful in the development of new TGR5 agonists.

2. Materials and methods

2.1. Common feature pharmacophore model

A pharmacophore is an abstract description of the structural features that are necessary for molecular recognition of a ligand by a biological macromolecule. In this study, the structures of the TGR5 agonists were selected in a manner that would ensure

[a]*Key Laboratory of Receptors-Mediated Gene Regulation and Drug Discovery, People's Hospital of Hebi, School of Medicine, Henan University, Henan, China. E-mail: hb_lwg@163.com*

[b]*Key Laboratory of Molecular Pathology, School of Basic Medical Science, Inner Mongolia Medical University, Hohhot, China*

[c]*Key Laboratory of Structure-Based Drug Design and Discovery, Ministry of Education, School of Pharmaceutical Engineering, Shenyang Pharmaceutical University, 103 Wenhua Road, Shenhe District, Shenyang 110016, PR China*

[d]*State Key Laboratory of Chemical Resource Engineering, College of Life Science and Technology, Beijing University of Chemical Technology, Beijing, China. E-mail: ydwangbuct2009@163.com*

† Electronic supplementary information (ESI) available. See DOI: 10.1039/d0ra10168k

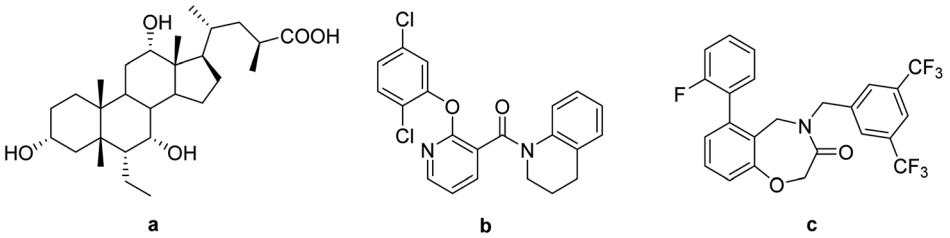

Fig. 1 Structures of some known TGR5 agonists.

that they were bioassayed under similar conditions. Nine representative TGR5 agonists with diverse scaffolds were chosen to form a training set (Fig. 2). The diverse conformations within the training set were taken as the input ligands to create pharmacophore hypotheses by using the 'Common Feature Pharmacophore Generation' module in the Discovery Studio program package. The common feature pharmacophore analysis was carried out using the HipHop program of Discovery Studio 3.0.

In this study, feature mapping revealed that hydrogen bond acceptor (A), hydrogen bond donor (D), hydrophobic group (H), and ring aromatic (R) could effectively map all agonists in the training set. The maximum pharmacophore hypotheses were set to ten. The minimum feature option was 4, and maximum feature option was 6. The principal and MaxOmit Feat values were assigned to these training set compounds (Table 1).The conformational models of the training set compounds were built using the "best conformer generation" method with a 10 kcal mol^{-1} energy threshold and the maximum conformation was set to 200. Maximum pharmacophore hypotheses was set to 10 and the minimum interfeature distance was set to 2.97 Å. All other parameters were set by default. Ten pharmacophore models were produced and the best one was selected for further study.

2.2. Pharmacophore validation

Decoy test method was used to evaluate the suitability of pharmacophore to identify TGR5 agonists. The decoy set consisted of 600 molecules which comprised of 30 known TGR5 agonists and 570 molecules with unknown activity randomly selected from the ZINC database. To compare a single pharmacophore to a set of ligands, we used the Ligand

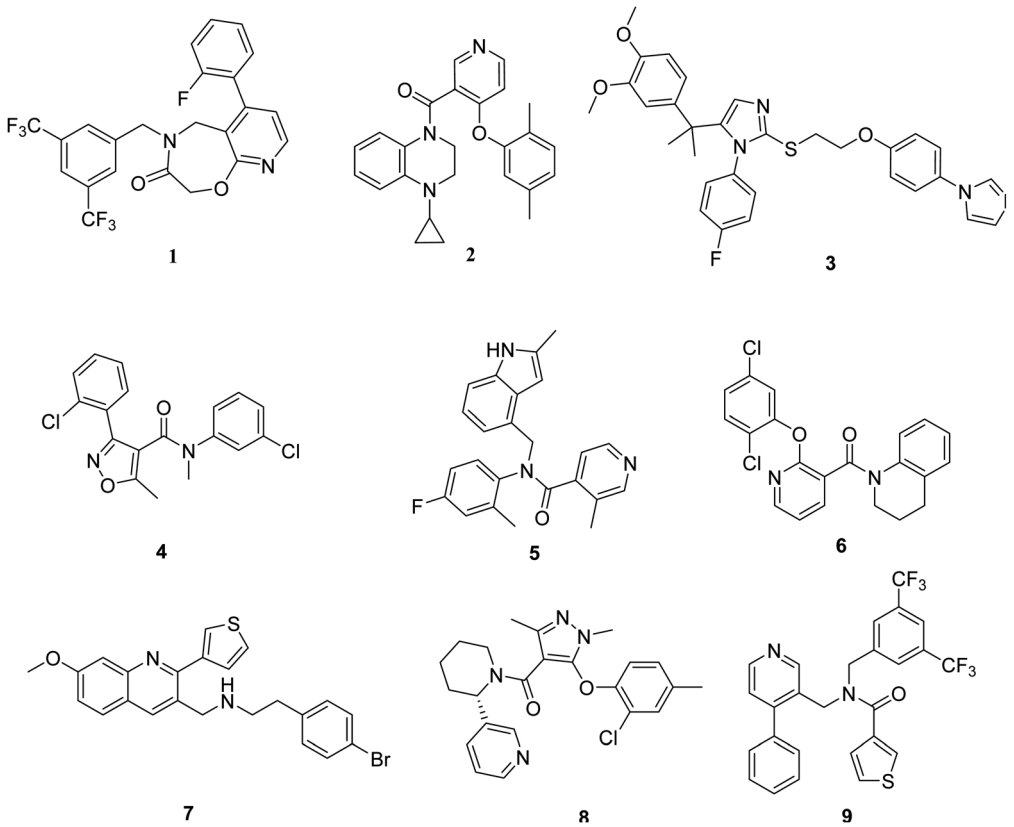

Fig. 2 The structure of training set compounds.

Table 1 *In vitro* TGR5 agonists activities of the selected compounds (EC_{50}, nM)

Name	EC_{50} (nM)	Principal	MaxOmitFeat	Ref.
1	0.23	2	0	13
2	0.72	2	0	13
3	0.057	2	0	16
4	6.8	1	1	17
5	9.72	1	1	18
6	10	1	1	13
7	82	1	1	19
8	113	1	1	20
9	120	1	1	21

Pharmacophore Mapping protocol. Ligand Pharmacophore Mapping module with best conformation generation and flexible fitting sets was used. We then calculated parameters such as total hits (Ht), active hits (Ha), % yield of actives (%*A*), % ratio of actives (%*Y*), enrichment factor (EF), and goodness of hit score (GH).

$$\%A = \frac{\mathrm{Ha}}{A} \times 100\%$$

$$\%Y = \frac{\mathrm{Ha}}{\mathrm{Ht}} \times 100\%$$

$$\mathrm{EF} = \frac{\mathrm{Ha}/\mathrm{Ht}}{A/D}$$

$$\mathrm{GH} = \frac{\mathrm{Ha}(3\mathrm{Ha} + \mathrm{Ht})}{4\mathrm{Ht} \times A} \times \left(1 - \frac{\mathrm{Ht} - \mathrm{Ha}}{D - A}\right)$$

Here, D is number of compounds, A is number of active compounds, Ht is number of hits retrieved, Ha is number of actives in hit list, %*A* is a ratio of actives retrieved in hit list, %*Y* is a fractions of hits relative to size of database (hit rate or selectivity), EF is enrichment factor, and GH is Güner–Henry score.

2.3. Molecular docking model

In order to evaluate the ligand interaction into TGR5 binding pocket, the molecular docking was carried out using the Schrödinger suite. A published crystal structure of P395 bound within the active site cavity of TGR5 (PDB ID:7CFM) with the resolution of 3.00 Å served as a useful template for the docking.[22] The TGR5 was prepared by the "protein preparation wizard" module in Maestro. Missing residues in the protein structure were reconstructed. Assigned bond orders to all bonds in the TGR5 structure including het groups and added hydrogens to all atoms. Remove the original hydrogens before adding hydrogens to the structure. The water molecules were removed and energy minimization was done using OPLS_2005 force field, restrained minimization with convergence of heavy atoms to an RMSD of 0.3 Å.

The "Receptor Grid Generation" module in Maestro is used to specify a receptor structure and set up the grid generation job. The binding site was defined as the site sphere of 15 Å radius around the original ligand P395 in the co-crystal structures. Ligands were prepared using "LigPrep" module in Maestro were minimized with OPLS-2005 force field. Ionization states were assigned at pH 7.0 ± 2, the chirality was retained, and the tautomers were generated. Finally, the "ligand docking" was carried out using the maestro based on the grid using standard precision (SP) and extra precision (XP) docking precision with ligands docked flexibly. The docked conformers were evaluated using GlideScore. All compounds were docked flexibly into binding site. In molecular docking, 5000 poses per ligand were generated for the initial phase of docking, out of which 800 best poses were chosen for energy minimization.

2.4. Cell-based TGR5 agonism assay

A lentivirus expressing human TGR5 (NM_001077191.1) was obtained from Hanbio Biotechnology Co. Ltd. HEK293T cells were transfected with lentivirus and a stable cell line was isolated using drug selection following standard techniques. LCA was used as reference compounds. The test compounds and reference compounds were prepared in DMSO at stock solutions of 10 mM. TGR5-mediated cAMP generation was assayed using a HTRF (Homogeneous Time-Resolved Fluorescence) detection method (HTRF cAMP dynamic 2 Assay Kit; Cisbio cat #62AM4PEB) according to the manufacturer's protocol. For agonist tests, 5 μl of cells were mixed with 5 μl of the test compound and incubated 30 min at room temperature in the white 384-well microplates. Then, 5 μl cAMP-d2 and 5 μl anti cAMP-cryptate in lysis buffer were added to each well followed by 1 hour incubation at room temperature. Signal was quantified on a CLARIOstar Microplate Reader (BMG LABTECH) and calculated using the equation (665 nm/620 nm) × 10 000.

Table 2 Summary of the pharmacophore models for TGR5 agonists

Hypothesis	Features[a]	Rank[b]	Direct Hit[c]	Partial Hit[d]	Max Fit
01	HHHHAA	114.816	111111111	000000000	6
02	HHHHAA	114.617	111111111	000000000	6
03	HHHHAA	114.425	111111111	000000000	6
04	RHHHHA	113.818	111111111	000000000	6
05	RHHHHA	113.251	111111111	000000000	6
06	HHHHAA	112.834	111111111	000000000	6
07	HHHHAA	112.513	111111111	000000000	6
08	HHHHAA	112.302	111111111	000000000	6
09	RHHHHA	112.286	110111111	001000000	6
10	RHHHHA	112.114	111111111	000000000	6

[a] H, hydrophobic group; A, hydrogen bond acceptor; R, ring-aromatic. [b] The ranking score of training set compounds fitting the hypothesis. [c] Direct Hit indicates whether ("1") or not ("0") a molecule in the training set mapped every feature in the hypothesis. [d] Partial Hit indicates whether ("1") or not ("0") a particular molecule in the training set mapped all but one feature in the hypothesis. Numeration of molecules is from right to left in both Direct Hit and Partial Hit.

Table 3 The validation results of the pharmacophore models

Hypothesis	*D*	*A*	Ht	Ha	%*A*	%*Y*[a]	EF	GH
01	600	30	72	28	93.3	38.9	7.78	0.47
02	600	30	56	30	100.0	53.6	10.71	0.62
03	600	30	76	24	0.8	31.6	6.32	0.35
04	600	30	46	30	100.0	65.2	13.04	0.72
05	600	30	66	28	93.3	42.4	8.48	0.49
06	600	30	80	26	86.7	32.5	6.50	0.39
07	600	30	76	26	86.7	34.2	6.84	0.40
08	600	30	74	26	86.7	35.1	7.03	0.41
09	600	30	64	30	100.0	46.9	9.38	0.57
10	600	30	69	28	93.3	40.6	8.12	0.48

[a] Here, *D* is number of compounds, *A* is number of active compounds, Ht is number of hits retrieved, Ha is number of actives in hit list, %*A* is a ratio of actives retrieved in hit list, %*Y* is a fractions of hits relative to size of database (hit rate or selectivity), EF is enrichment factor, and GH is Güner–Henry score.

3. Results and discussion

3.1. Common feature pharmacophore model and validation

The top-ten pharmacophore hypotheses were generated using this training set with scores ranging from 112.114 to 114.816 (Table 2). These hypotheses could be classified into two groups according to the pharmacophore features: HHHHAA (01, 02, 03, 06, 07, 08) and RHHHHA (04, 05, 09, 10). The hypotheses were classified by their locations and the direction of their features.

3.2. Pharmacophore validation

To further validate the final pharmacophore models, the Güner–Henry (GH) scoring method was used to identify the best pharmacophore model.[23,24] The decoy set consisted of 600 molecules which comprised of 30 known TGR5 agonists[20,25–31] and 570 molecules with unknown activity randomly selected from the ZINC database. The results of the decoy set validation are shown in Table 3. All of the 30 active molecules were successfully identified by hypothesis 02, hypothesis 04 and hypothesis 09, and the number of total hits were 56, 46 and 64, respectively. GH score higher than 0.7 suggests a very good and reliable model.[32,33] Hypothesis 04 possess an excellent GH score of 0.72. Thus, it can be indicating that the hypothesis 04 is a reliable model which may be valuable in identifying diverse active TGR5 agonists from the database.

Finally, hypothesis model 04 was selected as the optimal pharmacophore model. As shown in Fig. 3, hypothesis model 04 contained a six point pharmacophore containing one ring aromatic (R), four hydrophobic groups (H), and one H-bond acceptor (A), which were represented as orange, cyan, and green, respectively. The training set compound **3** can be matched to the pharmacophore model 04 (Fig. 3B).

3.3. Virtual screening

In order to identify novel TGR5 agonists, a multi-step virtual screening workflow including ligand-based pharmacophore screening, docking screening and finally a careful visual inspection of the molecules was performed. Firstly, the 323 842 compounds of the DrugBank, Specs, TargetMol and in our library databases were screened by Lipinski's rule filter to remove unreasonable molecules using DruLiTo software. Secondly, the validated ligand-based pharmacophore model Hypo04 was used to screen. Based on the fit values (≥2) for a compound matching against pharmacophore, resulting in 2045 screening hits kept in the chemical library. Thirdly, the

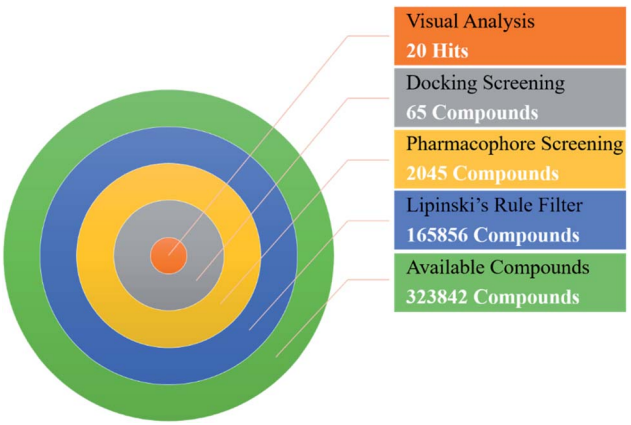

Fig. 4 Workflow of the virtual screening protocol.

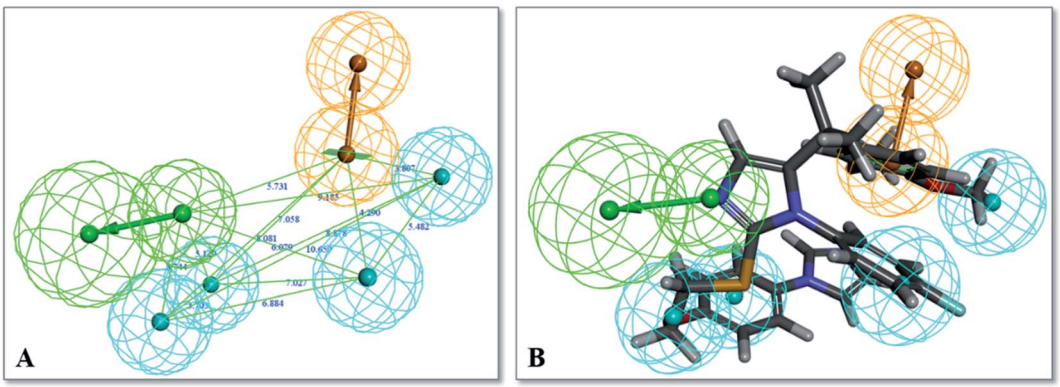

Fig. 3 (A) Selected common feature pharmacophore model 04 for TGR5 agonists consisting of one H-bond acceptor (A), four hydrophobic groups (H) and one ring aromatic (R). (B) Pharmacophore model 04 mapping with active compound **3**.

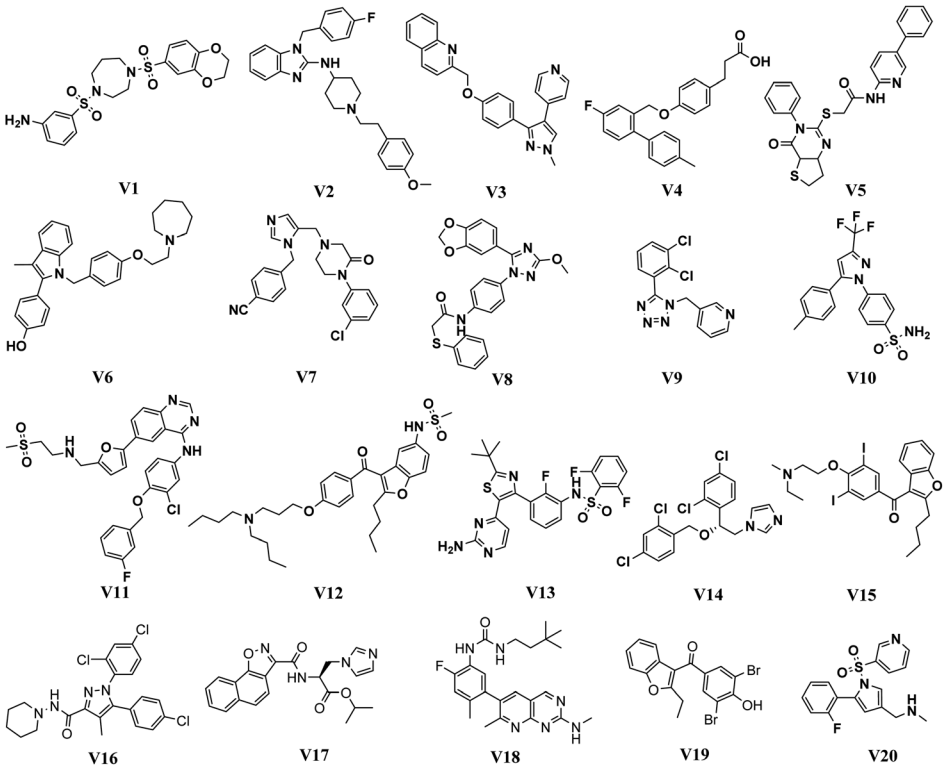

Fig. 5 Structures of 20 hits selected by virtual screening.

retrieved compounds from the pharmacophore search were saved as SD file and docked into the prepared receptor grid using standard precision (SP) and extra precision (XP) docking algorithm. The Glide XP scoring function was used to predict binding affinity between compounds and TGR5. According to the predicted binding energy (≤−6), top 65 compounds were picked out (see Tables S1 and S2†). The flowchart of the virtual screening is shown in Fig. 4. After careful visual inspection, 20 hit compounds (Fig. 5) were selected and purchased from Target Molecule Corp. for *in vitro* bioassay test.

3.4. *In vitro* biological evaluation

The selected compounds were evaluated for their ability to activate TGR5 by assessed for intracellular levels of cAMP. As reference compound, the response of LCA at 10 μM was defined as 100% TGR5 activation. Vehicle control with 0.1% DMSO was set to 0% TGR5 activation. As shown in Fig. 6, most compounds exhibited significant activity with more then 50% receptor activation at 40 μM. At 10 μM, only two compounds (**V12** and **V14**) achieved more than 40% receptor activation, but the remaining compounds less then 30%. The most potent compounds **V12** and **V14** were further evaluated using a dose–response experiment (see Fig. S1†). Compounds **V12** and **V14** displayed obvious TGR5 agonist activity, with the EC_{50} values of 19.5 μM and 7.7 μM, respectively.

3.5. Molecular docking analysis

In order to understand the binding mode, the most active compound **V14** was docked into the active site of TGR5 by using the Glide XP. A published crystal structure of P395 bound within the active site cavity of TGR5 (PDB ID:7CFM) with the resolution of 3.00 Å served as a useful template for the docking. The docking conformations within the catalytic site of TGR5 are displayed in Fig. 7A.

Compound **V14** maps on the pharmacophore model 04 are shown in Fig. 7B. Compound **V14** maps well on the pharmacophore feature hydrophobic feature (H), hydrogen bond acceptor (A), and aromatic ring (R). The imidazole group which mapped as hydrogen bond acceptor (A) was able to make hydrogen bond interactions with Thr243 and Ser247. The 2,4-dichloroaniline moiety which was mapped as aromatic ring (R) made pi–pi interactions with Phe96 and hydrophobic feature (H) with the surrounding residues Phe96, Glu169, Leu174. 2,4-Dichlorobenzyl alcohol moiety of the compound is a hydrophobic group, it can forms hydrophobic interaction with Leu74, Trp75, Pro92, which maps well on the pharmacophore feature hydrophobic feature (H).

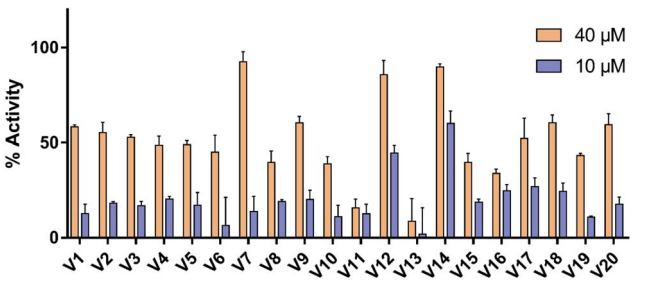

Fig. 6 Result of the preliminary bioassay screening. The response to 10 μM LCA was set to 100%.

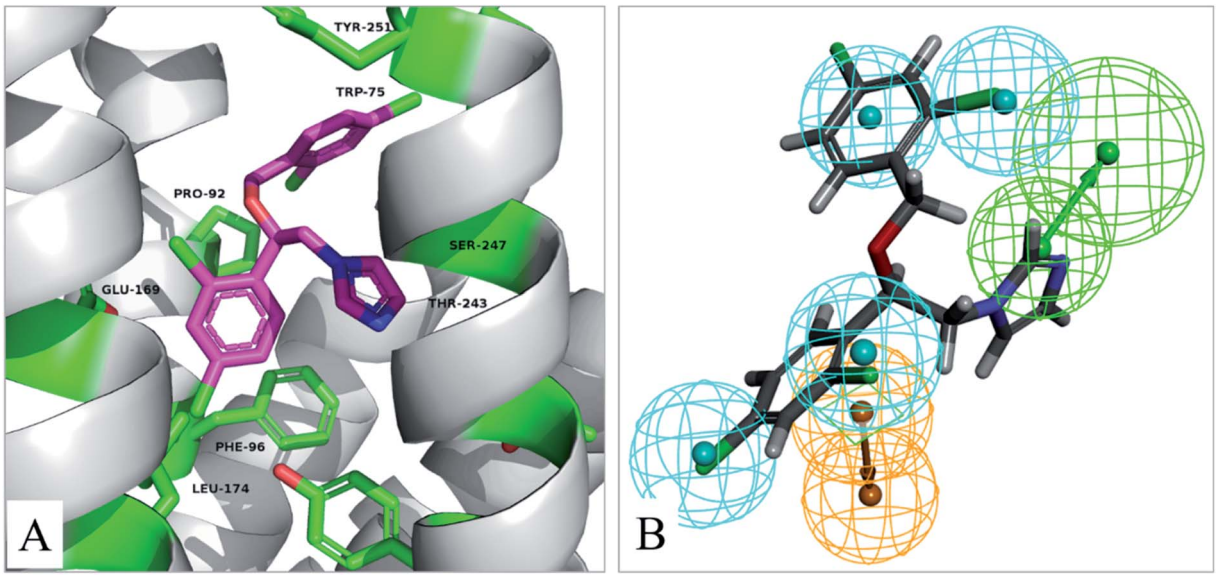

Fig. 7 (A) The binding mode of compound **V14** in the active site of TGR5 (PDB ID:7CFM). (B) Pharmacophore model 04 mapping with active compound **V14**.

4. Conclusion

TGR5 has emerged as an important and attractive therapeutic target for the treatment of metabolic disorders, such as non-alcoholic steatohepatitis, type 2 diabetes mellitus (T2DM), and obesity. Computational technique like virtual screening as been successfully applied for the generation of hit and lead structure candidates.

To understand the mechanism of action of TGR5 agonists, common feature pharmacophore models were generated and molecular docking was performed. These models provided more detailed information and better descriptions of ligand binding. The common feature pharmacophore model consists of six chemical features (RHHHHA): one ring aromatic (R), four hydrophobic groups (H), and one hydrogen acceptor (A). Finally, ligand-based virtual screening combined with pharmacophore mapping and molecular docking was performed to identify novel nonsteroidal TGR5 agonists. Twenty compounds were selected for *in vitro* biological evaluation, and results showed that most compounds exhibited between 50% and 80% receptor activation at 40 μM. Among these compounds, **V12** and **V14** displayed obvious TGR5 agonist activity, with the EC_{50} values of 19.5 μM and 7.7 μM, respectively. Compounds **V12** and **V14** could be considered potential TGR5 agonist candidate and also may be used as initial hits for developing novel TGR5 agonists.

Conflicts of interest

There are no conflicts to declare.

Acknowledgements

This work is supported by the National Natural Science Foundation of China (Grant No. 81970726 and No. 81472232), Henan Provincial Natural Science Foundation (Grant No. 182300410323), First Class Discipline Cultivation Project of Henan University (Grant No. 2019YLZDYJ19) and Plan for Scientific Innovation Talent of Henan Province (Grant No. 154100510004), Key Program for Science & Technology from Henan Education Department (Grant No. 21A310001) to W. -D. C., the National Natural Science Foundation of China (Grant No. 81903444), China Postdoctoral Science Foundation (Grant No. 2018M640674) and Key Science, Technology Program of Henan Province (Grant No. 192102310145) and Henan Postdoctoral Foundation (Grant No. 201902027) to S. Z., Major Scientific and Technological Innovation Project of Hebi to R. H., the National Natural Science Foundation of China (Grant No. 81970551 and No. 81672433) and the Fundamental Research Funds for the Central Universities and Research projects on biomedical transformation of China-Japan Friendship Hospital (Grant No. PYBZ1803) to Y. -D. W.

References

1 T. Maruyama, Y. Miyamoto, T. Nakamura, Y. Tamai, H. Okada, E. Sugiyama, T. Nakamura, H. Itadani and K. Tanaka, *Biochem. Biophys. Res. Commun.*, 2002, **298**, 714–719.
2 Y Kawamata, R. Fujii, M. Hosoya, M. Harada, H. Yoshida, M. Miwa, S. Fukusumi, Y. Habata, T. Itoh and Y. Shintani, *J. Biol. Chem.*, 2003, **278**, 9435–9440.
3 G. Vassileva, A. Golovko, L. Markowitz, S. J. Abbondanzo, M. Zeng, S. Yang, L. Hoos, G. Tetzloff, D. Levitan and N. J. Murgolo, *Biochem. J.*, 2006, **398**, 423.
4 M. Watanabe, S. M. Houten, C. Mataki, M. A. Christoffolete, B. W. Kim, H. Sato, N. Messaddeq, J. W. Harney, O. Ezaki and T. Kodama, *Nature*, 2006, **439**, 484–489.
5 T. Maruyama, K. Tanaka, J. Suzuki, H. Miyoshi, N. Harada, T. Nakamura, Y. Miyamoto, A. Kanatani and Y. Tamai, *J. Endocrinol.*, 2006, **191**, 197–205.

6 J. E. Campbell and D. J. Drucker, *Cell Metab.*, 2013, **17**, 819–837.
7 S. Katsuma, A. Hirasawa and G. Tsujimoto, *Biochem. Biophys. Res. Commun.*, 2005, **329**, 386–390.
8 G. Musso, M. Cassader, F. D. Michieli, F. Rosina, F. Orlandi and R. Gambino, *Hepatology*, 2012, **56**, 933–942.
9 A. L. Birkenfeld and G. I. Shulman, *Hepatology*, 2014, **59**, 713–723.
10 J. Abrigo, F. Gonzalez, F. Aguirre, F. Tacchi, A. Gonzalez, M. P. Meza, F. Simon, D. Cabrera, M. Arrese, S. Karpen and C. Cabello-Verrugio, *J. Cell. Physiol.*, 2021, **236**, 260–272.
11 S. Li, M. Qiu, Y. Kong, X. Zhao, H. J. Choi, M. Reich, B. H. Bunkelman, Q. Liu, S. Hu, M. Han, H. Xie, A. Z. Rosenberg, V. Keitel, T. H. Kwon, M. Levi, C. Li and W. Wang, *J. Am. Soc. Nephrol.*, 2018, **29**, 2658–2670.
12 R. Pellicciari, A. Gioiello, A. Macchiarulo, C. Thomas, E. Rosatelli, B. Natalini, R. Sardella, M. Pruzanski, A. Roda and E. Pastorini, *J. Med. Chem.*, 2009, **52**, 7958–7961.
13 H. Duan, M. Ning, X. Chen, Q. Zou, L. Zhang, Y. Feng, L. Zhang, Y. Leng and J. Shen, *J. Med. Chem.*, 2012, **55**, 10475.
14 K. A. Evans, B. W. Budzik, S. A. Ross, D. D. Wisnoski, J. Jin, R. A. Rivero, M. Vimal, G. R. Szewczyk, C. Jayawickreme and D. L. Moncol, *J. Med. Chem.*, 2009, **52**, 7962–7965.
15 R. J. Hodge and D. J. Nunez, *Diabetes, Obes. Metab.*, 2016, **18**, 439–443.
16 S. Agarwal, A. Patil, U. Aware, P. Deshmukh, B. Darji, S. Sasane, K. V. Sairam, P. Priyadarsiny, P. Giri and H. Patel, *ACS Med. Chem. Lett.*, 2015, **7**, 51.
17 B. W. Budzik, K. A. Evans, D. D. Wisnoski, J. Jin, R. A. Rivero, G. R. Szewczyk, C. Jayawickreme, D. L. Moncol and H. S. Yu, *Bioorg. Med. Chem. Lett.*, 2010, **20**, 1363–1367.
18 K. Hogenauer, L. Arista, N. Schmiedeberg, G. Werner, H. Jaksche, R. Bouhelal, D. G. Nguyen, B. G. Bhat, L. Raad, C. Rauld and J. M. Carballido, *J. Med. Chem.*, 2014, **57**, 10343–10354.
19 D. W. Piotrowski, K. Futatsugi, J. S. Warmus, S. T. M. Orr, K. D. Freeman-Cook, A. T. Londregan, L. Q. Wei, S. M. Jennings, M. Herr, S. B. Coffey, W. H. Jiao, G. Storer, D. Hepworth, J. Wang, S. Y. Lavergne, J. E. Chin, J. R. Hadcock, M. B. Brenner, A. C. Wolford, A. M. Janssen, N. S. Roush, J. Buxton, T. Hinchey, A. S. Kalgutkar, R. Sharma and D. A. Flynn, *ACS Med. Chem. Lett.*, 2013, **4**, 63–68.
20 A. T. Londregan, D. W. Piotrowski, K. Futatsugi, J. S. Warmus, M. Boehm, P. A. Carpino, J. E. Chin, A. M. Janssen, N. S. Roush, J. Buxton and T. Hinchey, *Bioorg. Med. Chem. Lett.*, 2013, **23**, 1407–1411.
21 J. J. Zhu, M. M. Ning, C. Guo, L. N. Zhang, G. Y. Pan, Y. Leng and J. H. Shen, *Eur. J. Med. Chem.*, 2013, **69**, 55–68.
22 F. Yang, C. Mao, L. Guo, J. Lin, Q. Ming, P. Xiao, X. Wu, Q. Shen, S. Guo, D.-D. Shen, R. Lu, L. Zhang, S. Huang, Y. Ping, C. Zhang, C. Ma, K. Zhang, X. Liang, Y. Shen, F. Nan, F. Yi, V. C. Luca, J. Zhou, C. Jiang, J.-P. Sun, X. Xie, X. Yu and Y. Zhang, *Nature*, 2020, **587**, 499–504.
23 M. M. Liu, L. Zhou, P. L. He, Y. N. Zhang, J. Y. Zhou, Q. Shen, X. W. Chen, J. P. Zuo, W. Li and D. Y. Ye, *Eur. J. Med. Chem.*, 2012, **52**, 33–43.
24 R. J. Li, Y. L. Wang, Q. H. Wang, J. Wang and M. S. Cheng, *Comput. Math. Methods Med.*, 2015, **2015**, 11.
25 S. Agarwal, A. Patil, U. Aware, P. Deshmukh, B. Darji, S. Sasane, K. V. V. M. Sairam, P. Priyadarsiny, P. Giri, H. Patel, S. Giri, M. Jain and R. C. Desai, *ACS Med. Chem. Lett.*, 2016, **7**, 51–55.
26 H. L. Duan, M. M. Ning, Q. A. Zou, Y. L. Ye, Y. Feng, L. N. Zhang, Y. Leng and J. H. Shen, *J. Med. Chem.*, 2015, **58**, 3315–3328.
27 B. W. Budzik, K. A. Evans, D. D. Wisnoski, J. Jin, R. A. Rivero, G. R. Szewczyk, C. Jayawickreme, D. L. Moncol and H. Yu, *Bioorg. Med. Chem. Lett.*, 2010, **20**, 1363–1367.
28 J. Zhu, M. Ning, C. Guo, L. Zhang, G. Pan, Y. Leng and J. Shen, *Eur. J. Med. Chem.*, 2013, **69**, 55–68.
29 Q. Zou, H. Duan, M. Ning, J. Liu, Y. Feng, L. Zhang, J. Zhu, Y. Leng and J. Shen, *Eur. J. Med. Chem.*, 2014, **82**, 1–15.
30 D. P. Phillips, W. Q. Gao, Y. Yang, G. B. Zhang, I. K. Lerario, T. L. Lau, J. Q. Jiang, X. Wang, D. G. Nguyen, B. G. Bhat, C. Trotter, H. Sullivan, G. Welzel, J. Landry, Y. L. Chen, S. B. Joseph, C. Li, W. P. Gordon, W. Richmond, K. Johnson, A. Bretz, B. Bursulaya, S. F. Pan, P. McNamara and H. M. Seidel, *J. Med. Chem.*, 2014, **57**, 3263–3282.
31 H. L. Duan, M. M. Ning, X. Y. Chen, Q. A. Zou, L. M. Zhang, Y. Feng, L. N. Zhang, Y. Leng and J. H. Shen, *J. Med. Chem.*, 2012, **55**, 10475–10489.
32 C. Jang, D. K. Yadav, L. Subedi, R. Venkatesan, A. Venkanna, S. Afzal, E. Lee, J. Yoo, E. Ji, S. Y. Kim and M. H. Kim, *Sci. Rep.*, 2018, **8**, 21.
33 A. Zeb, M. Son, S. Yoon, J. H. Kim, S. J. Park and K. W. Lee, *Comput. Struct. Biotechnol. J.*, 2019, **17**, 579–590.